An electrodynamic trap with an advanced geometry used for evaporation rate measurements of single water droplets

C. Heinisch[1,*], J. Petter[1], N. Damaschke[2], T. Tschudi[1], C. Tropea[3]
[1]Institute of Applied Physics, Darmstadt University of Technology,
Hochschulstr. 6, 64289 Darmstadt, Germany
[2]Institute of General Electrical Engineering, University of Rostock,
Albert-Einstein-Str. 2, 18051 Rostock, Germany
[3]Chair of Fluid Mechanics and Aerodynamics, Darmstadt University of Technology,
Petersenstr. 30, 64287 Darmstadt, Germany

Abstract
We present an electrodynamic trap with an advanced geometry providing 360° optical access in the horizontal plane and a channel for a gas stream. Calculations of the electric field show points of stable trapping and how the stability of the trapping can be redistributed between the axial and radial direction. Using this trap the evaporation rate of single water droplets in stagnant and flowing nitrogen with a temperature of 20°C was measured successfully. The evaporation rate in stagnant nitrogen is compared with theory.

Introduction

Droplets in sprays and aerosols play an important role in the environment and industry, for example in combustion engines, in the atmosphere, in spray dryers and aerosol, drug delivery. An important part of our understanding of the fundamentals of these processes is based on the contact free investigation of single droplets enabled by the development of levitation techniques and a broad spectrum of optical measurement techniques. This work contributes to the advancement of electrodynamic levitation, also known as Paul trap, ion trap, electrodynamic trap, electrodynamic balance or electrodynamic chamber, which offers an alternative to optical levitation or acoustic levitation. Electrodynamic levitation is especially interesting as it is well suited for droplets of a diameter between 10 µm and 300 µm, corresponding to typical droplet sizes in the aforementioned applications. In contrast to the optical levitation the electrodynamic levitation is not restricted to transparent samples. Compared to the acoustic levitation no additional perturbing flow is induced. Moreover, the work verifies experimental data of the evaporation of water droplets in stagnant nitrogen at 20°C, where little experimental data has been published up to now: Taflin et al. [1] show only four data points for these parameters.

The mass transfer of evaporating droplets in a gas flow can be described by the change of the overall Sherwood number ($\overline{Sh}$). There are different known dependences of the Sherwood number at small Reynolds numbers (Re), for example Ranz and Marshall [2], who studied the evaporation of water droplets suspended on a feed capillary in dry air for Re > 2. The Sherwood numbers found by Beard and Pruppacher [3], who studied the evaporation of water droplets in a wind tunnel for 0.1<Re<350, are up to 15% lower than those of Ranz and Marshall. The electrodynamic levitation in comparison to the wind tunnel allows choosing the velocity of the gas independent from the current droplet size. Recent studies of Smolik et al. [4] of droplets suspended on a thermocouple in a flow of air at 1<Re<200 show even up to 15% lower Sherwood numbers than those of Beard and Pruppacher for 1<Re<10. This comparison shows that further investigations are required. In this contribution we demonstrate the successful levitation of water droplets of diameters between 20 and 50 µm for the measurement of the evaporation rate in a nitrogen gas flow of up to 110 ml/min. This corresponds to an estimated Reynolds number of Re = 5. In contrast to the suspension of droplets the heat and mass transfer is not disturbed by the suspending capillary [2] or wire [4] in the electrodynamic trap. Moreover in the electrodynamic trap it is not necessary to adapt the velocity of the gas to the droplet size during evaporation in contrast to the levitation in a wind tunnel [3].

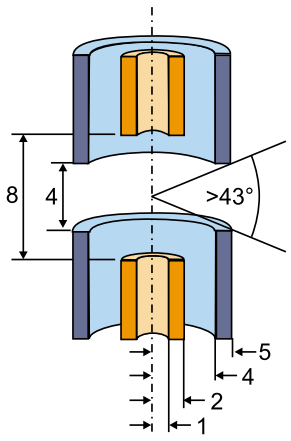

Fig. 1: Cross section of the electrodes of the electrodynamic trap. (Dimensions are given in millimeters.)

* Corresponding author: christian.heinisch@physik.tu-darmstadt.de

An electrodynamic trap with an advanced geometry

One disadvantage of electrodynamic levitation is the electrodes limiting the optical access. Therefore a new kind of geometry of the electrodes providing a horizontal 360° view to the sample has successfully been developed. The electrodes used in the first electrodynamic trap for particles by Wuerker et al [5] create an ideal electric potential, but they cover most of the interior of the trap and complicate the optical investigation of the samples. To overcome this problem, the new geometry as shown in fig. 1 was developed consisting of four electrodes in the form of tubes: two opposed inner and two opposed outer electrodes.

Different geometries have been reviewed by Davis and Schweiger [6]. The known geometries provide either not 360° optical access in the horizontal plane or less than 43° continuous access in vertical direction (e.g. disc electrodes) or the stability of the droplet trapping under the same conditions is smaller (for example double ring electrode). An example for the latter can be seen comparing fig. 2 and 3 showing the absolute value of the calculated electric field. This figure is interpreted as follows: The principle of electrodynamic trapping is based on an electric potential of the form of a saddle oscillating with time. In the centre of the trap the electric field is zero. Where the electric field is not zero, the charged droplet or particle is oscillating. Depending on the gradient of the electric field, the force on the droplet changes during each oscillation. This leads to a mean force on the droplet, responsible for the stability of the droplet. This mean force can be represented by the pseudo potential

$$\varphi \propto qE^2 / \omega^2 ,$$

where q is the charge of the droplet, E the electric field and ω the oscillation frequency of the field. Fig. 2 shows the absolute field value of the electric field in the cross section of the trap with the advanced geometry presented here. The minima of the electric field in the centre and inside the upper and lower inner electrode are points for stable trapping, but only the centre is used. The height of the pseudo potential well and thus the maximum of the absolute value of the electric field |E| around the minimum can be seen as a measure for the stability of the trapping in the sense of how much kinetic energy a droplet can have without leaving the trap. In fig. 2 the maximum of |E| on the z-axis is 289 kV/m at z = 3.3 mm and 59 kV/m on the r-axis at r = 2.7 mm. The corresponding values for the double ring trap in fig. 3 are 65 kV/m and 85 kV/m, respectively. In the sum this is less than half. The dimensions of the electrodes in fig. 3 were chosen to provide the same range of optical access from the side. Moreover, in fig. 3 the gradient of the absolute value of the electric field close to the centre is smaller than in fig. 2. This influences the stability in the sense of how far moves the droplet from the centre under small perturbations, for example in a turbulent flow. The stability in this sense can be quantified by the coefficient c_1 of the squared term $z^2-r^2/2$ in a series expansion of the electric potential. $c_1 = 3.5 \cdot 10^{-4}$ V/m^2 for fig. 2 and $c_1 = 0.47 \cdot 10^{-4}$ V/m^2 for fig. 3 speaks clearly in favour of the four tube trap.

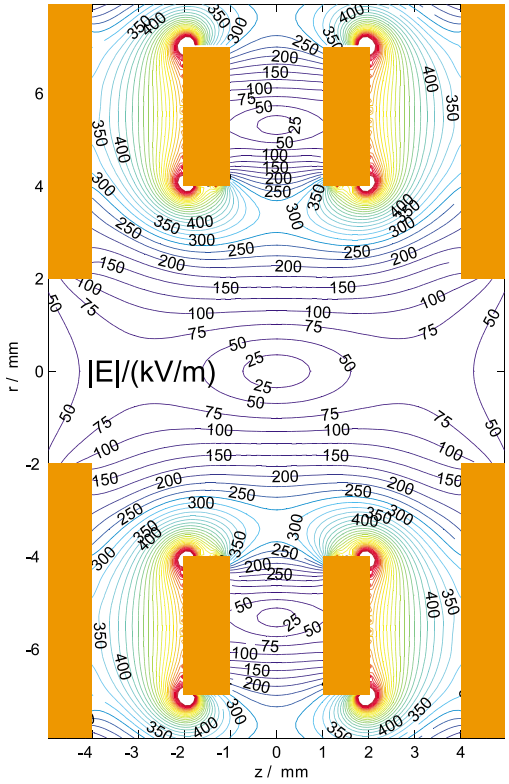

Fig. 2: Calculated absolute value of the electric field in the cross-section of the electrodes of the electrodynamic trap for a potential of 1 kV at the inner electrodes and ground potential at the outer electrodes. The minimum at the centre is used for stable trapping of the droplet.

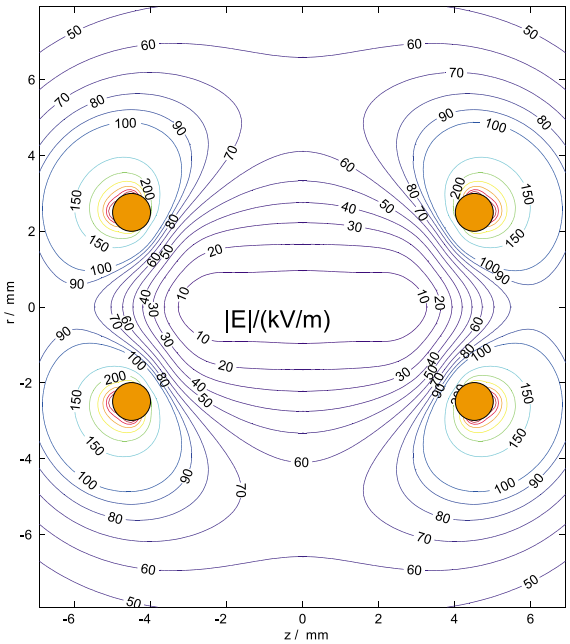

Fig. 3: Calculated absolute value of the electric field in the cross-section of the electrodes of a two ring trap, when a potential of 1 kV is applied to both rings.

Fig. 4 shows the same electrodes as in fig. 2 but with a distance reduced by 2 mm. This changes the maximum electric field to |E|=270 in the z-axis and |E|=122 kV/m on the r-axis. This demonstrates how the stability on the r-axis can be increased at the expense of the stability on the z-axis.

These theoretical investigations above demonstrate that concerning the stability of the droplet the geometry of the four tubes is superior to other geometries with the same angular range of optical access. Moreover, the ratio of the stability in r- and z-axis can be adapted to our needs by approaching the electrodes.

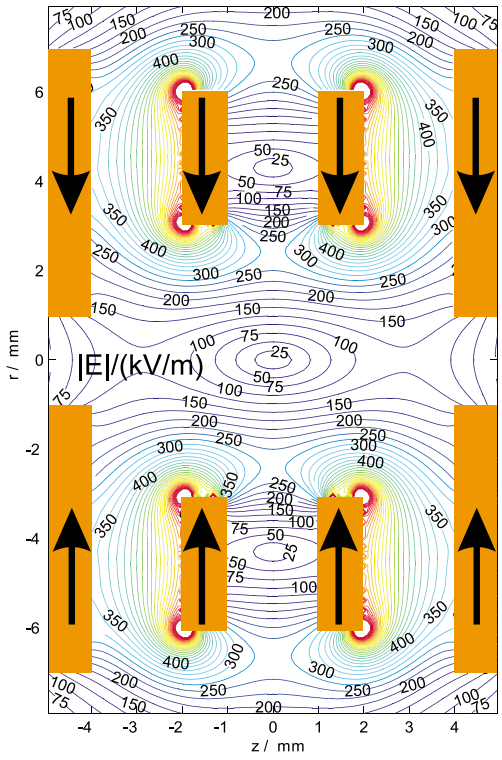

Fig. 4: Calculated electric field with the distance between upper and lower electrodes reduced by 2 mm in comparison to fig. 2.

Evaporation model

For the evaporation of single water droplets of less than 50 µm in stagnant nitrogen at 20°C, we consider the following evaporation model based on Maxwell [7]:

- mass transport only by diffusion (neglecting Stefan flow and convection by buoyancy)
- partial pressure of water vapour at the droplet surface equal to the saturation vapour pressure
- homogeneous droplet temperature
- ideal gas law for nitrogen and water vapour
- constant diffusivity and heat conductivity of the gas phase (for temperature T_{ref}=2/3 T_S + 1/3 T_{inf}, where T_S is the temperature at the droplet surface and T_{inf} far from the droplet)
- energy balance between the heat transported from the bulk gas to the droplet and the heat of evaporation (no radiation)
- quasi-stationary

This results in the so called D^2-law predicting a droplet surface decreasing linear with time [6]:

$$D^2(t) = D_0^2 - \beta_D t$$

The energy balance

$$\dot{m}(t) h_{vap} = \dot{Q}(t),$$

where h_{vap} is the latent heat of vaporization, relates the mass transfer rate $\dot{m}(t)$ and the heat transfer rate $\dot{Q}(t)$ leading to the droplet temperature called wet bulb temperature below the ambient temperature. For the numerical calculation we used the following constants:

- latent heat of vaporization at temperature T_S=4.4 °C (ref. [8]): $h_{i,vap}$=2.490·10^6 J/kg
- diffusion constant for water vapor in air at temperature T_{ref}=9.6 °C (ref. [9]): D_{ij}=2.36·10^{-5} m^2/s·(1±7%)
- heat conductivity of the gas phase at T_{ref}=9.6 °C (linear interpolation from ref. [10]): κ=0.0247 W/(K m) (1±2%)
- density of the liquid phase (ref. [10]): ρ=1000 kg/m^3
- saturation water vapor pressure according to Goff-Gratch (ref. [10])

For the ambient gas temperature of T_{inf}=(20±1) °C this results in a wet bulb temperature of T_S=(4.4±0.7) °C and finally in the evaporation rate β_D=(12.4±0.7)·10^{-10} m^2/s.

For this calculation the choice of the temperature for evaluation of the diffusion constant and the heat conductivity of the gas phase is important. Using the Droplet surface temperature results in β_D =12.1·10^{-10} m^2/s, using the ambient temperature in β_D =12.9·10^{-10} m^2/s. In our case the rule T_{ref} =2/3 T_S + 1/3 T_{inf} was applied as a rule of thumb. For higher precision more detailed numerical calculations have to be done.

Experimental Setup

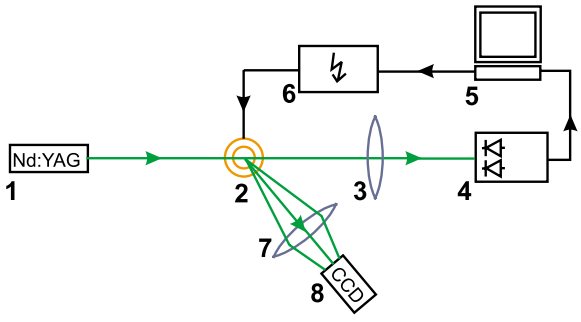

Fig. 5: Experimental setup for measuring the evaporation rate of single water droplets: 1, Nd:YAG laser at 532 nm wavelength, continuous wave; 2, electrodynamic trap; 3, lens; 4, segmented photo diode; 5, computer with DA/AD-card; 6, high voltage amplification; 7, lens; 8, CCD camera

The setup used to measure evaporation rates is shown in fig. 5. The electrodynamic trap (2) presented above is used to levitate a single water droplet, generated by a HP 51604A inkjet cartridge. The electrodes are enclosed in a chamber of 50 mm x 50 mm x 20 mm with glass windows at the sides. A Nd:YAG laser (1) with 15 mW output power and a wavelength of 532 nm illuminates the droplet. Using a lens (3) the droplet is imaged on a segmented photodiode (4) in order to detect the vertical position of the droplet. The signal of the segmented photodiode is evaluated by a PC (5) controlling the AC and DC voltage of the electrodes via a separate high voltage amplification (6). The light scattered by the droplet is detected by a CCD camera (8) placed in the focal plane of a lens (7). In this way the angular intensity distribution around the droplet is recorded on 20 x 1392 pixels in the range between 45° and 57° with a rate of 126 images per second. Before the measurement the chamber is flooded with nitrogen with a volume share of water less than $3 \cdot 10^{-5}$. The volume flow rate of nitrogen for measuring droplets in a flow was determined by a floating element flow meter.

The stripe pattern recorded by the CCD camera is analysed after averaging over all lines. The mean angular distance of the stripes is used to calculate the diameter of the droplet according to the formula of Glantschnig and Chen [11] with a known refractive index n=1.333. This formula is based on geometrical optics.

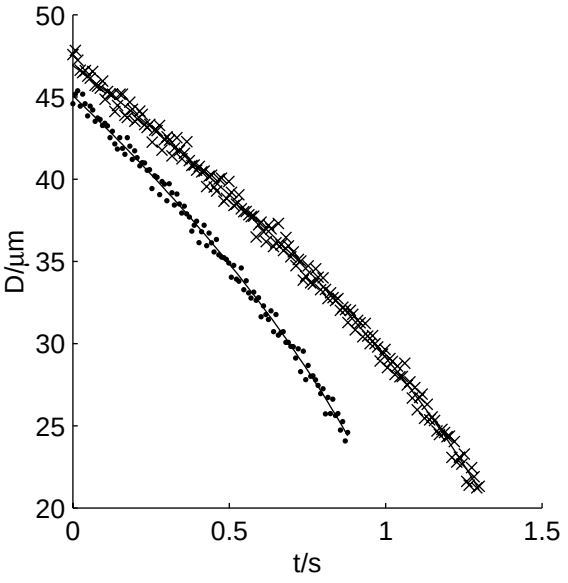

Fig. 6: Diameter d of water droplets as a function of time measured in stagnant nitrogen (crosses), in flowing nitrogen (dots). The fitting of the theoretical D^2-law (solid line) yields an evaporation rate of $\beta_D=13.5 \cdot 10^{-10}$ m^2/s and $\beta_D=16.4$•10-10 m^2/s respectively.

Results and Discussion

The measured diameter of the droplet in stagnant nitrogen as a function of time is shown in fig. 6 with crosses. Fitting the D2-law

$$D(t) = \sqrt{D_0^2 - \beta_D t}$$

to the experimental data between D=47 µm and D=27 µm yields the evaporation rate $\beta_D=13.5 \cdot 10^{-10}$ m^2/s. The theoretical prediction of $\beta_D=12.4 \cdot 10^{-10}$ m^2/s and the result of Taflin et al. [1] are within 8% in agreement with our results.

Moreover, the evaporation of water droplets in flowing nitrogen is shown in fig. 6 with dots. The evaporation rate is significantly increased for a flow rate of 110 ml/min. Also this data can be fitted to the to D^2-law yielding an evaporation rate of $\beta_D=16.4 \cdot 10^{-10}$ m^2/s. Assuming a Poiseuille flow inside the inner electrodes and using an expression from Schlichting [12] for a free jet between the lower and upper electrodes allows rough estimation of the velocity at the centre to 2.4 m/s and the Reynolds number to Re=5. A precise calibration of the velocity as a function of the flow rate has still to be carried out. The velocity of the gas stream was limited due to the response time of the control loop for the droplet position. Higher velocities can be probably reached by using an analog PID controller and by further adjustment of its parameters. These results demonstrates the successful levitation of water droplets in flowing nitrogen at low Reynolds numbers for the measurement of the evaporation rate using Mie scattering in the presented advanced electrodynamic trap.

Conclusion

We presented a new geometry of an electrodynamic trap providing 360° optical access in the horizontal plan and more than 43° in the vertical direction. This allows easier and more flexible measurements. Theoretical calculations of the electric field show better stability of the sample for this geometry in comparison with a two ring electrode of comparable dimensions. Further calculations show that the stability of the sample can be redistributed in horizontal and vertical direction according to our needs by varying the distance between the upper and lower electrodes. This electrodynamic trap was successfully combined with an optical measurement technique: the size of evaporation water droplets was measured by the analysis of the Mie scattering. In this way the evaporation rate of water in stagnant nitrogen has been measured at an ambient temperature of 20°C. The result is in agreement with theory within 8%. Therewith the theory could be verified at these parameter settings, where only little experimental data has been published. Within the uncertainty of the used diffusion constant for water in air, we could not see a difference to the diffusion constant of water in nitrogen.

Moreover, the evaporation rate of water droplets in flowing nitrogen was measured successfully up to a flow rate of 110 ml/min and an evaporation rate of

$\beta_D=16.4\cdot10^{-10}$ m^2/s. These results are promising to obtain a dependence of the Sherwood number on the Reynolds number using this advanced electrodynamic trap after calibration of velocity versus flow rate.

Acknowledgements

This work is funded by the German Research Foundation in the frame of the Research Training Group 1114 "Optical Techniques for Measurement of Interfacial Transport Phenomena". We thank Dr. Franco Laeri and Mr. Atacan Erodabasi for the development and the provision of a cubic Paul trap and the used high voltage components and Belal Al-Zaitone for discussions.

References

1. Daniel C. Taflin, S. H. Zhang, Theresa Allen and E. James Davis, Measurement of droplet interfacial phenomena by light-scattering techniques, *AIChE Journal*, vol. 34, pp. 1310-1320, 1988

2. W. E. Ranz and W. R. Marshall, Evaporation from drops 2, *Chemical Engineering Progress*, vol. 48, pp. 173-180, 1952

3. K. V. Beard and H. R. Pruppacher, A Wind Tunnel Investigation of the Rate of Evaporation of Small Water Drops Falling at Terminal Velocity in Air, *Journal of the Atmospheric sciences*, vol. 28, pp. 1455-1464, 1971

4. Jiri Smolik, Lucie Dzumbova, Jaroslav Schwarz and Markku Kulmala, Evaporation of ventilated water droplet: connection between heat and mass transfer, *Aerosol Science*, vol. 32, pp. 739-748, 2001

5. R. F. Wuerker, H. Shelton and R.V. Langmuir, Electrodynamic Containment of Charged Particles, *J. Appl. Phys.*, vol. 30, pp. 342-349, 1959

6. E. James Davis and Gustav Schweiger, *The Airborne Microparticle*, Springer, Berlin, 2002

7. J. C. Maxwell, Diffusion, 1877 in: W. D. Niven, *J. C. Maxwell Scientific Papers*, Cambridge, 1890

8. Horst Stöcker, *Taschenbuch der Physik: Formeln, Tabellen, Übersichten*, 3. ed., Deutsch, Thun, Frankfurt am Main, 1998

9. Landolt and Börnstein, *Zahlenwerte und Funktionen aus Physik, Chemie, Astronomie, Geophysik und Technik, II. Bd. Eigenschaften der Materie in ihren Aggregatzuständen, 5. Teil: Transportphänomene, Kinetik, Homogene Gasgleichgewichte*, 6. ed., Springer, Berlin, 1969

10. G. Fischer (ed.), *Zahlenwerte und Funktionen aus Naturwissenschaft und Technik/ Landolt-Börnstein, Gruppe 5. Geophysik und Weltraumforschung, Bd. 4 Meteorologie, Teilbd. B. Physikalische und Chemische Eigenschaften der Luft*, Springer, Berlin, 1988

11. W. J. Glantschnig and S. H. Chen, Light scattering from water droplets in the geometrical optics approximation, *Applied Optics*, vol. 20, pp. 2499-2509, 1981

12. Herrmann Schlichting and Klaus Gersten, *Boundary layer theory*, Springer, Berlin, 2000